Bitlis Eren Üniversitesi Fen Bilimleri Dergisi
BİTLİS EREN UNIVERSITY JOURNAL OF SCIENCE
ISSN: 2147-3129/e-ISSN: 2147-3188
VOLUME: 12 NO: 3 PAGE: 625-633 YEAR: 2023
DOI:10.17798/bitlisfen.1251421

Investigation of Copper-Iron Oxide Thin Film Grown by Co-Sputtering

Sevda SARİTAS[1*]

[1] *Atatürk University, Department of Electric Power Generation, Transmission and Distribution, İspir Hamza Polat Vocational College, Erzurum, Turkey.*
(*ORCID: 0000-0002-7274-3968*)

Keywords: Copper oxide, Iron oxide, Thin film, Co-sputtering,

Abstract

In this study, the iron oxide and copper oxide structures were grown with the DC magnetron and RF magnetron sputtering respectively and the $Cu_xFe_{3-x}O_4$ structure was grown with the co-sputtering. Structural optical and topographic examination of the grown thin films has been done in detail. Absorption measurements of the thin films were taken with the help of a Perkin Elmer UV/Visible Lambda 2S spectrometer at room temperature. The value of the band gap energy with the fit drawn in the $(ahυ)^2$ (cm^{-1} eV^2) counter energy graph of Fe_2O_3, $Cu_xFe_{3-x}O_4$, Cu_2O thin film is grown on glass was calculated as 2.44, 2.39, 2.55 eV respectively. Also, the structural and topographic properties of thin film structures were investigated by scanning electron microscopy (SEM), atomic force microscopy (AFM), X-ray diffraction (XRD), X-ray photoelectron spectroscopy (XPS), and Raman spectroscopy. According to XPS results; the binding energies of the 2p3\2 orbital for the Fe^{3+} (Fe_2O_3) ion is 710.85 eV and for the Fe^{3+} ($Cu_xFe_{3-x}O_4$) ion is 712.49 eV. The binding energy of the 2p3\2 orbital for the Cu^{1+} (Cu_2O) ion is 933.64 eV, and for the Cu^{2+} ($Cu_xFe_{3-x}O_4$) ion is 935.58 eV. O^{2-} the binding energy of the 1s orbital of the ions are 529.95, 531.35 and 529.39 eV for Fe_2O_3, $Cu_xFe_{3-x}O_4$, and Cu_2O respectively.

1. Introduction

For a long time, extensive studies have been carried out on the optical, magnetic, and electrical properties of many nanostructures that are important for scientific, technological, environmental security, cyber security, industrial and medical applications [1], [2]. Evaluation of nano-scale events with nanotechnology and the development of similar ones with applications have created new perspectives in science. In terms of optical, magnetic, thermal, electrical and mechanical properties, nano-sized particles have quite different properties than micron-sized particles and are more advantageous [3]-[5]. These advantages include applications in different fields such as energy, environmental biology, catalyst, magnetic and gas sensors, and electromagnetic interference problems. It has a very important place in applications such as imaging, magnetic recording, magnetic cooler and magnetic printers.

Iron is the most abundant metal on earth. This element has played a role in the development of our civilization, as in Antiquity, as the basis of numerous structural materials. Corrosion processes associated with iron oxides (excluding pigment applications) and iron oxide have long been considered a nuisance. However, in recent years, iron oxides have become increasingly studied materials as extremely useful materials in various fields such as medicine, biology, catalysis, photovoltaics, and combustible gas sensors [6]-[12].

As a metal oxide, CuO attracts attention due to its low cost and intense solar absorption, which can be found in abundance in nature. However, CuO has been reported to be a profitable and promising nanomaterial for applications such as gas sensors, batteries, catalysis, semiconductor photovoltaic cells, field emission, and photocatalytic reactions. The CuO structure is grown with very different growth techniques such

*Corresponding author: sevda.saritas@atauni.edu.tr
Received: 14.02.2023, Accepted: 16.09.2023

as electrospin [13], e-beam evaporation, wet chemical methods [14]-[16], microwave heating technique [17], electropolymerization [18], and hydrothermal method [19]. CuO is an important monoclinic semiconductor with a narrow band gap in the (1.2-1.9 eV) range, an important structure used in solar cell and sensor technology. In addition, CuO is a p-type semiconductor material and worldwide research is carried out by researchers [20]-[22]. Copper oxide and iron oxide thin films are ideal materials in terms of band gap, especially in solar cell applications. The band gap of the films changes by changing the growth parameters (power, growth pressure, oxygen partial pressure, substrate temperature, etc.) [23].

Cations such as Cr, Co, Ni, Cu, Zn, and Ag can be located in interstitial sites and tetrahedral places instead of Fe cation with appropriate cation distribution in Fe_2O_3. Thus, changes can occur in the electronic and magnetic properties of maghemite [24]. Iron oxide and copper oxide structures may differ in terms of optical and structural properties, depending on the growth technique and growth parameters. Copper oxide and iron oxide thin films are ideal materials in terms of band gap, especially in solar cell applications. The band gap of the films grown by the sputter technique changes by changing the growth parameters (power, growth pressure, oxygen partial pressure, substrate temperature, etc.). The main applications of CuO are in optoelectronic and high-performance electronic devices [25]. CuO belongs to antiferromagnetic materials and has a different crystal system [17]. Besides, the bandgap is not a single value but a range of values from 1.75 eV up to 2.45eV. Copper vacancies in CuO play an important role in hole conduction [26], [27], [17], [28]. As an important semiconductor metal oxide, hematite (α-Fe_2O_3) is the most stable phase of iron oxide under ambient conditions [29]. α-Fe_2O_3, which is an n-type semiconductor with an indirect band gap of 2.2 eV, is regarded as an attractive material due to its applications in photoelectrochemical devices [30], photocatalysts [31], magnetic materials [32], pigments, anticorrosive agents and sensors [33].

Recent studies have shown the availability of Fe_2O_3/CuO composite structures [34]-[36], which aim to enhance the absorption range in solar cell research. Adjusting the band gap is crucial for numerous optical applications. In this study, our objective is to obtain three distinct structures. The first two structures are commonly used in optical and solar cell applications, while the third structure is a novel combination of the first two. This study aims to demonstrate the impact of magnification techniques on various aspects of a structure, including its structural, optical, morphological, and topographic features. Additionally, the study aims to highlight how adjusting magnification parameters can lead to the creation of more practical and beneficial structures.

So, it is aimed to show that thin films can be grown in a wide band range, especially by changing the growth parameters of the copper iron oxide structure grown by the co-sputtering technique. In this study, the iron oxide and copper oxide structures were grown with the DC magnetron, RF magnetron sputter technique respectively, and the $Cu_xFe_{3-x}O_4$ structure was grown with the co-sputtering. Structural optical and topographic examination of the grown thin films has been done in detail.

2. Material and Method

The iron oxide and copper oxide structures were grown with the DC magnetron and RF magnetron sputter technique respectively, and the $Cu_xFe_{3-x}O_4$ structure was grown with the co-sputtering.

The sputter technique is the growth of ions, atoms and molecules broken from the metal target on the heated substrate cleaned by chemical processes as a thin film with the help of inert gas. To break the material to be grown from the metal target, argon is turned into an inert gas carrier plasma with the help of an RF or DC power source and the plasma performs the detachment process by beating the surface of the target metal. The copper sputtering foil target has 2 inches (dia) x 0.005 inches (thickness) and the iron sputtering foil target has 2 inches (dia) x 0.005 inches (thickness). An iron target was placed in the DC power gun and a copper target was placed in the RF gun source. The sputter technique has been preferred because it is a reproducible, relatively low cost, and low surface roughness film growth technique that can more easily control the optical and structural properties of the grown film. In the sputter technique, due to the vacuum environment, the pollution rate is lower and higher quality binary and triple compounds are grown.

In this experimental study, an iron thin foil was attached to the DC power supply and a copper metal foil target was attached to the RF power supply part. While the DC power supply is 120 watts, the RF power supply is set to 40 watts. The glass substrates placed for the vacuum chamber up to $5*10^{-6}$ Torr pressure (base pressure) were heated up to 450 degrees. Then 100 sscm of inert argon gas

was sent in and plasma was formed. Then, 40 sscm of argon and 3 sscm of oxygen gas were given to grown pressure of $8.5*10^{-3}$ Torr and growth was made for 35 minutes. Also, the copper oxide and iron oxide films grown on glass substrates at 8 mTorr grown pressure.

In this study, the structural, optical, and topographic properties of copper iron oxide structures grown by RF-DC co-sputtering were investigated by scanning electron microscopy (SEM), atomic force microscopy (AFM), X-ray diffraction (XRD), X-ray photoelectron spectroscopy (XPS) and UV-VIS spectroscopy and Raman spectroscopy.

3. Results and Discussion

One of the most used methods to determine the optical absorption edge and band gap of semiconductors is the absorption measurement method. Absorption measurements of the thin films on the glass substrate were taken with the help of Perkin Elmer UV/Visible Lambda 2S spectrometer at room temperature. The spectrometric measurement range used is 300–900 nm. In the measurements (Figure 1a) made, information about the band gap of (Figure 1b) the material was obtained.

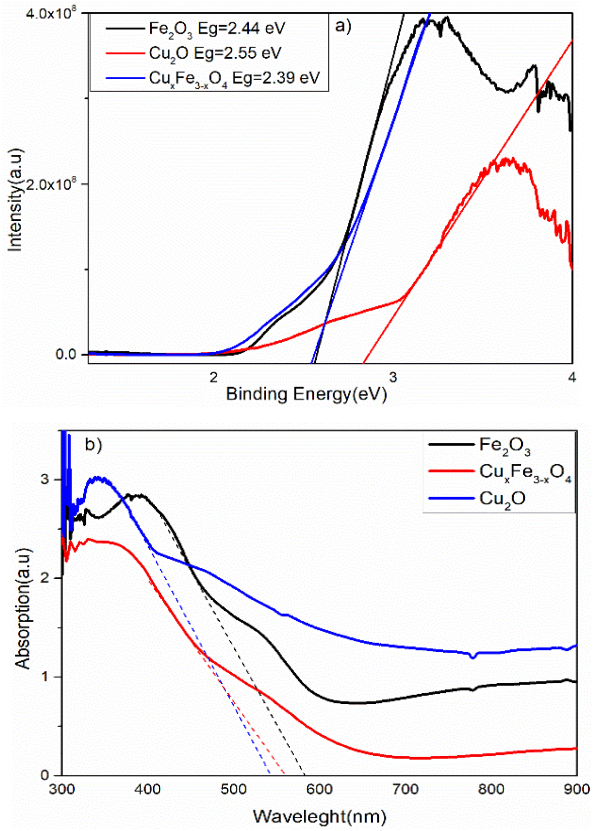

Figure 1. **a)** Absorption measurements of the Fe_2O_3, $Cu_xFe_{3-x}O_4$, Cu_2O thin films, **b)** the value of the band gap energy with the fit drawn in the $(ah\upsilon)^2$ (cm^{-1} eV^2) counter energy graph of Fe_2O_3, $Cu_xFe_{3-x}O_4$, Cu_2O

In Figure 1b, the value of the band gap energy with the fit drawn in the $(ah\upsilon)^2$ (cm^{-1} eV^2) counter energy graph of Fe_2O_3, $Cu_xFe_{3-x}O_4$, Cu_2O thin film grown on glass was calculated as 2.44, 2.39, 2.55 eV. This value of the iron oxide film is compatible with the literature for maghemite and hematite phases. While the Fe_2O_3 and Cu_2O thin films absorb at smaller wavelengths, shifts are observed at larger wavelengths as a result of doping. This may mean that the imperfections in the structure cause the energy gap to shrink, as it creates the possibility of transition at the band gab edge.

The XRD diffraction pattern of the iron oxide, structure growing on the glass substrate is given in Figure 2 and it has been determined that the structure has a tetragonal structure. The lattice constants have the values a=b=8.34 $\dot{A}$, c=25.02 $\dot{A}$ [JCPDS 39-1346]. Cu_2O (Figure 2a) has been determined that the structure has a cubic structure [JCPDS 45–0937] and the lattice constants have the values a=b=c= 4.26 $\dot{A}$ [37]. Two distinct peaks were observed, among which the characteristic maghemite and hematite peaks with orientations of 35.84 and 18.65 degrees. Also, two distinct peaks were observed, which are the characteristic cuprite peaks with orientations of 36.5° and 42.40° [JCPDS 05–0667 and 45–0937]. The values of the three peaks obtained in the XRD analysis (Figure 2a) results show that there is a polycrystalline structure for $Cu_xFe_{3-x}O_4$ thin film [38].

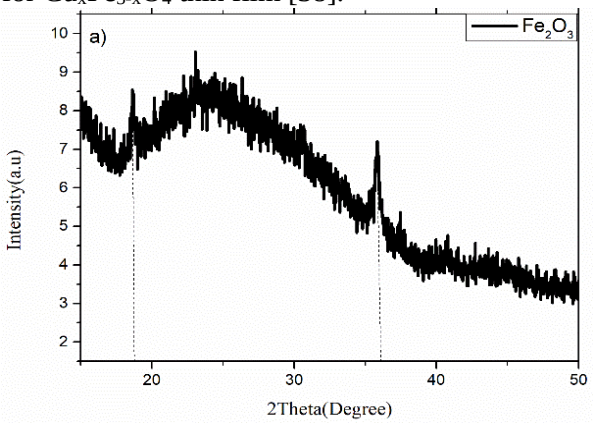

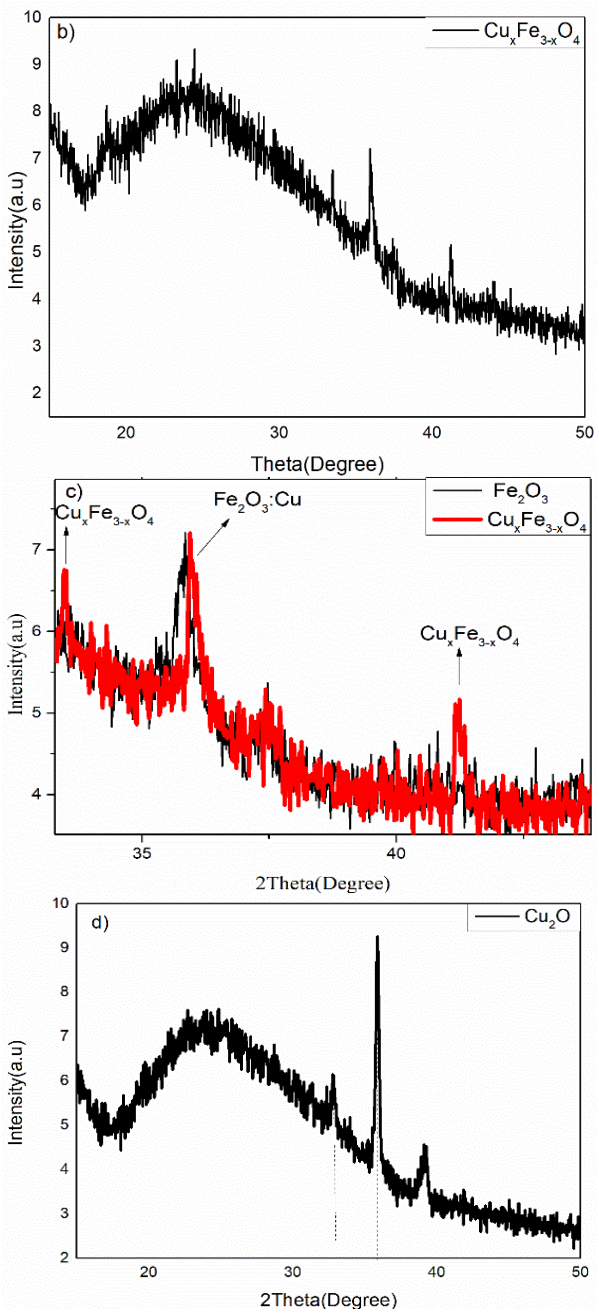

Figure 2. The XRD diffraction pattern of the **a)** Fe_2O3 b) Cu_xFe_2-xO3 **c)** $Cu_xFe_{3-x}O_4$, Fe_2O_3 and **d)** Cu_2O

In Cu cation-doped ferrites ($Cu_xFe_{3-x}O_4$), oxygen ions are replaced by Cu^{1+} and Fe^{3+} ions and have a tetragonal and cubic strong packing arrangement in two different crystallographies. In a published study, researchers tried to understand how Cu atoms change the structure properties of maghemite with Raman measurements. They revealed the active modes of five Raman spectra at room temperature, which are compatible with previous Raman spectra. The Raman active mode for Fe_2O_3 shifted (Figure 3) from 670 cm^{-1} for doped $Cu_xFe_{3-x}O_4$ to 660 cm^{-1} in the Raman spectrum with Cu doping and Cu doping density function [39], [40]. In line with their results, the researchers suggested that Cu^{1+} ions are mostly located in interstitial sites places [23].

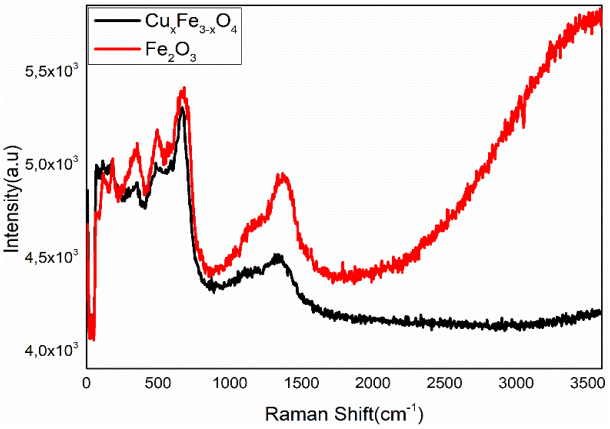

Figure 3. Raman shift graph of Fe_2O_3 and $Cu_xFe_{3-x}O_4$ structure

Figure 3 shows the stretching vibration mode of the Fe_2O_3 film. Peaks showing the Raman shift are seen. It can be said that these peaks are relatively narrow and intense and show Raman active states belonging to hematite phases [41], [42].

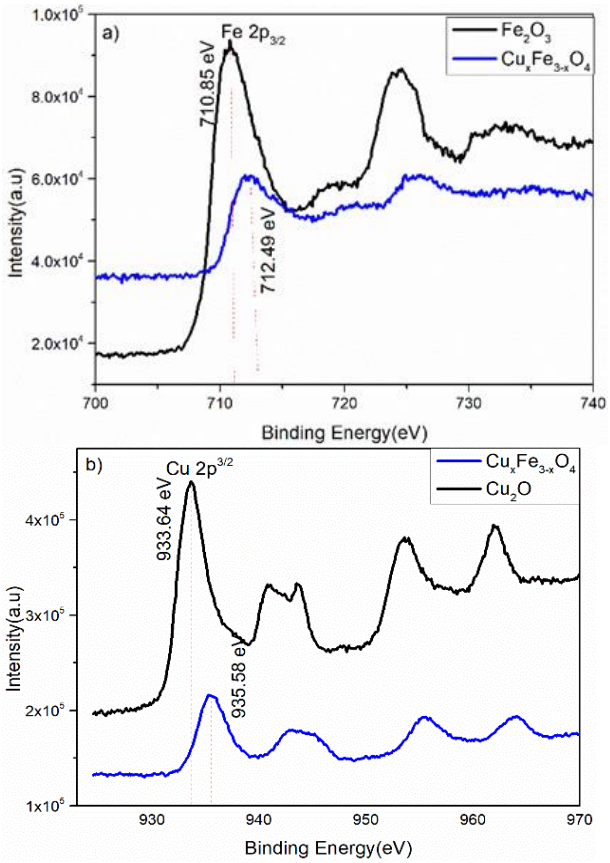

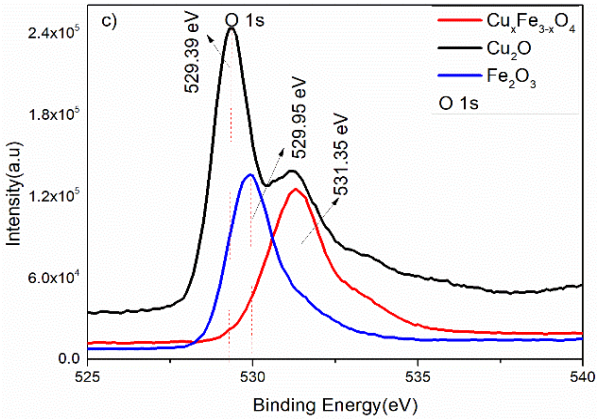

Figure 4. The binding energies of a) Fe^{3+}, b) Cu^{2+} and c) O^{-2} ions

As seen in Figure 4a, the binding energies of the 2p3\2 orbital for the Fe^{3+} (Fe_2O_3) ion are 710.85 eV and the binding energies of the 2p3\2 orbital for the Fe^{3+} ($Cu_xFe_{3-x}O_4$) ion are 712.49 eV. O^{2-} the binding energy of the 1s orbital of the ion is 529.95, and 531.35 eV for Fe_2O_3, $Cu_xFe_{3-x}O_4$ respectively. In Figure 4b, the binding energies of the 2p3\2 orbital for the Cu^{1+} (Cu_2O) ion are 933.64 eV, and the binding energies of the 2p3\2 orbital for the Cu^{2+} ($Cu_xFe_{3-x}O_4$) ion are 935.58 eV. In Figure 4c, O^{2-} the binding energy of the 1s orbital of the ion is 529.95, 531.35 and 529.39 eV for Fe_2O_3, $Cu_xFe_{3-x}O_4$, Cu_2O respectively. The peak intensities, which are an indicator of the number of bonding electrons, are very close to each other and the number of non-bonding electrons is low, which can be seen as the reason for its insulating property. In addition, we can say that its conductivity is low because the amount of oxygen and carbon with the atomic percentage of copper-iron oxide is high and it causes less oxygen vacancies that cause conductivity [41].

As seen in Figure 4(a, b, c), the graph showing the binding energies of Fe^{3+}, Cu^{2+}, and O^{2-} ions of the $Cu_xFe_{3-x}O_4$ compound, although the atomic oxygen amount is almost the same as in the Fe_2O_3 compound, there has been a decrease in the number of bonding oxygen electrons and hence the intensity of the peak. The reason for this situation can be thought that Cu may have bonded with Fe_2O_3 as well and some Cu may have bonded with O [42].

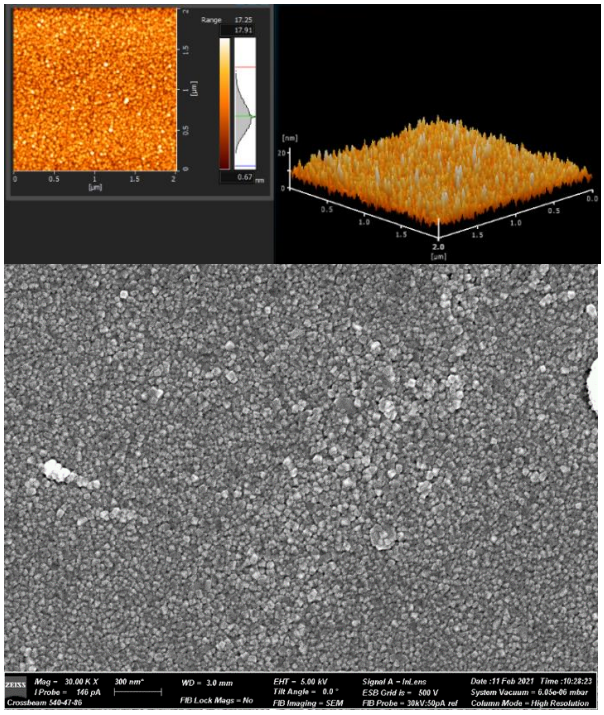

Figure 5. 2D and 3D AFM images and SEM images of the Fe_2O_3

The surface morphology of the iron oxide thin films was analyzed using the non-contact mode of AFM. Figure 5 shows 2D and 3D AFM images of the iron oxide films grown on glass substrates at 8.5 mTorr-grown pressure. The roughness values of the film are Ra= 1.88 nm and Sa=2.09 nm. In the SEM image (Fig. 5), it is seen that the structure is homogeneously distributed on the surface. In addition, a dark surface layer is observed, and under it, lighter colored structures with tetragonal shapes are observed.

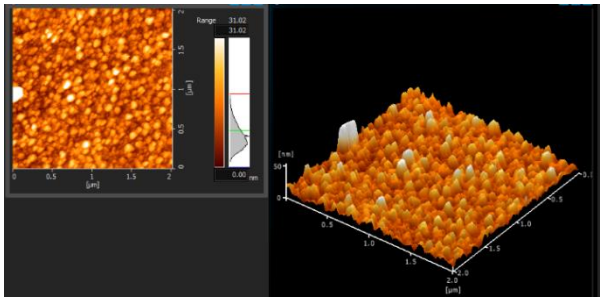

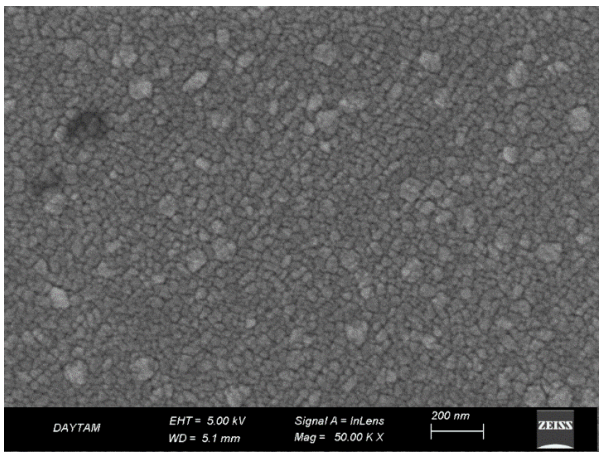

Figure 6. 2D and 3D AFM images and SEM images of the $Cu_xFe_{3-x}O_4$

The surface morphology of the copper-iron oxide thin films was analyzed using the non-contact mode of AFM. Figure 6 shows 2D and 3D AFM images of the copper-iron oxide films grown on glass substrates at 8.5 mTorr grown pressure. The roughness values of the film are Ra= 4.83 nm and Sa=4.19 nm. In the SEM (Fig. 6) image, it is seen that the structure is homogeneously distributed on the surface. In addition, a dark surface layer is seen, on which lighter colored structures are seen as lumps.

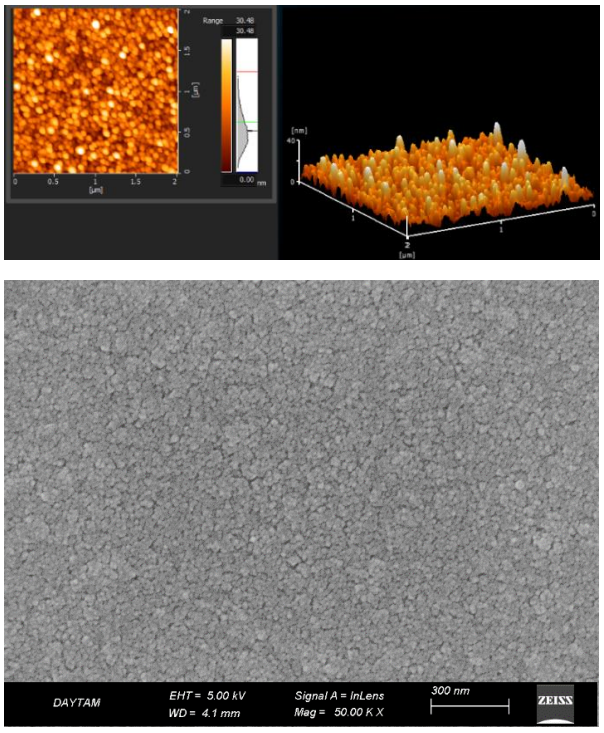

Figure 7. 2D and 3D AFM images and SEM images of the Cu_2O

The surface morphology of the copper oxide thin films was analyzed using the non-contact mode of AFM. Figure 7 shows 2D and 3D AFM images of the copper oxide films grown on glass substrates at 8 mTorr grown pressure. The roughness values of the film are Ra= 4.44 nm and Sa=4.10 nm. In the SEM image, it is seen that the structure is homogeneously distributed on the surface. In addition, relatively smaller-sized structures are observed.

Iron oxide and copper oxide structures may differ in terms of optical and structural properties, depending on the growth technique and growth parameters in terms of band gap, especially in solar cell applications. In this study, aims to show that thin films can be grown in a wide band range, especially by changing the growth parameters of the copper iron oxide structure grown by the co-sputter technique.

Structural optical and topographic examination of the grown thin films has been done in detail. The value of the band gap energy with the fit drawn in the $(ah\upsilon)^2$ ($cm^{-1}eV^2$) counter energy graph of Fe_2O_3, $Cu_xFe_{3-x}O_4$, Cu_2O thin film grown on glass was calculated as 2.44, 2.39, 2.55 eV. The binding energies of the 2p3\2 orbital for the Fe^{3+} (Fe_2O_3) ion are 710.85 eV and the binding energies of the 2p3\2 orbital for the Fe^{3+} ($Cu_xFe_{3-x}O_4$) ion are 712.49 eV. The binding energies of the 2p3\2 orbital for the Cu^{1+} (Cu_2O) ion are 933.64 eV, and the binding energies of the 2p3\2 orbital for the Cu^{2+} ($Cu_xFe_{3-x}O_4$) ion are 935.58 eV. O^{2-} the binding energy of the 1s orbital of the ion is 529.95, 531.35 and 529.39 eV for Fe_2O_3, $Cu_xFe_{3-x}O_4$, and Cu_2O respectively.

The band gap of the iron-copper oxide structure differs from that of the iron oxide and copper oxide structures and exhibits a value that falls between the two energy levels. This is consistent with the result reported in the literature, which suggests that doping induces a change in the forbidden band gap. SEM and AFM results show that the structures are homogeneously distributed across the surface. Angular or oval shapes are clearly visible. It can be observed that the contribution has taken on a new structural form. Additionally, the alteration in surface roughness reinforces this scenario. The changes in peak angles and intensities observed in the XRD results suggest the formation of a new crystal structure.

As can be seen from the XPS and Raman results, chemical bond changes in the iron oxide and copper oxide structures show that the desired thin film is grown. In all SEM images, they are seen that the structure is homogeneously distributed on the surface. The roughness values of $Cu_xFe_{2-x}O_3$

film are Ra= 4.83 nm and Sa=4.19 nm and these roughness values are bigger than others.

4. Conclusion and Suggestions

The band gap values of 2.44 and 2.55 eV in the films grown by the sputter technique. These results are different from the literature and it can be said that the growth parameters and the growth technique are quite effective. The change of the band gap (2.39 eV) of the iron copper oxide structure grown by the co-sputtering technique is a natural process, but it indicates a useful method for band gap engineering. In addition, it can be said that it is a useful method to produce materials with suitable band gaps for solar cells. Especially by combining the optical and structural properties of binary and ternary compounds, paves the way for the production of materials that will work more efficiently.

Acknowledgment

The present work was supported by Ataturk University. We would like to thank the Eastern Anatolia High Technology Application and Research Center (DAYTAM) for their support.

Conflict of Interest Statement

The authors have no relevant financial or non-financial interests to disclose. The author declare that they have no known competing financial interests or personal relationships that could have appeared to influence the work reported in this paper.

Statement of Research and Publication Ethics

The author declare that she has no conflict of interest

References

[1] C. Sanchez, B. Julián, P. Belleville, and M. Popall, "Applications of hybrid organic–inorganic nanocomposites," *J. Mater. Chem.*, vol. 15, no. 35–36, p. 3559, 2005.
[2] V. Bogush, "Application of Electroless Metal Deposition for Advanced," *Composite Shielding Materials. J. Optoelec. and Adv. Mat*, vol. 7, pp. 1635–1642, 2005.
[3] S. Kamiyama, K. Okamoto, and T. Oyama, "Study on regulating characteristics of magnetic fluid active damper," *Energy Convers. Manag.*, vol. 43, no. 3, pp. 281–287, 2002.
[4] D. D. L. Chung, "Electromagnetic interference shielding effectiveness of carbon materials," *Carbon N. Y.*, vol. 39, no. 2, pp. 279–285, 2001.
[5] L. X. Lian, L. J. Deng, and M. Han, "Microwave Electromagnetic and Absorption Properties of Nd2Fe14B/ -Fe Nanocomposites in the 0.5-18 and 26.5-40 GHz Ranges," *J. App. Phy*, vol. 101, pp. 09M – 520, 2007.
[6] U. Schwertmann and R. M. Cornell, *Iron Oxides in the Laboratory: Preparation and Characterization*, New York: Wiley, 2007.
[7] M. Vallet-Regí, C. V. Ragel, and A. J. Salinas, "Glasses with medical applications," *Eur. J. Inorg. Chem.*, vol. 2003, no. 6, pp. 1029–1042, 2003.
[8] A. N. Sukach, A. S. Lebedinskii, V. I. Grishchenko, and T. D. Lyashenko, "Effect of magnetic nanoparticles Fe3O4 on viability, attachment, and spreading of isolated fetuses and newborn rats," *Cell and Tissue Biology*, vol. 5, pp. 388–396, 2011.
[9] L. Levy, Y. Sahoo, K.-S. Kim, E. J. Bergey, and P. N. Prasad, "Nanochemistry: Synthesis and characterization of multifunctional nanoclinics for biological applications," *Chem. Mater.*, vol. 14, no. 9, pp. 3715–3721, 2002.
[10] A. Duret and M. Graetzel, "Visible light-induced water oxidation on mesoscopic α-Fe2O3 films made by ultrasonic spray pyrolysis," C*hemInform*, vol. 36, no. 48, 2005.
[11] J. Sartoretti, C. Ulmann, M. Alexander, B. D. Augustynski, and J. Weidenkaff, "Photoelectrochemical oxidation of water at transparent ferric oxide film electrodes," *Chemical Physics Letters*, vol. 376, 2005.
[12] W. B. Ingler Jr, J. P. Baltrus, and S. U. M. Khan, "Photoresponse of p-type zinc-doped iron(III) oxide thin films," *J. Am. Chem. Soc.*, vol. 126, no. 33, pp. 10238–10239, 2004.
[13] R. Sahay, J. Sundaramurthy, P.S. Kumar, V. Thavasi, S. G. Mhaisalkar, and S. Ramakrishna, "Synthesis and characterization of CuO nanofibers, and investigation for its suitability as blocking

layer in ZnO NPs based dye sensitized solar cell and as photocatalyst in organic dye degradation," *Journal of Solid State Chemistry*, 186, 261-267, 2012.

[14] Q. Liu, S. Anandan, S. H. Yang, and W. K. Ge, "Nanostructured CuO films on copper: Fabrication and application as a cathode in dye-sensitized TiO_2 solar cells," *in 2006 IEEE 4th World Conference on Photovoltaic Energy Conference* (Vol. 1, pp. 229-232). IEEE, 2006.

[15] T. Jiang, M. Bujoli-Doeuff, Y. Farré, Y. Pellegrin, E. Gautron, M. Boujtita, and F. Odobel, "CuO nanomaterials for p-type dye-sensitized solar cells," *RSC advances*, vol. 6, no. 114, pp. 112765-112770, 2016.

[16] S. Anandan, X. Wen, and S. Yang, "Room temperature growth of CuO nanorod arrays on copper and their application as a cathode in dye-sensitized solar cells," *Materials Chemistry and Physics*, vol. 93, no. 1, pp. 35-40, 2005.

[17] D. Wongratanaphisan, K. Kaewyai, S. Choopun, A. Gardchareon, P. Ruankham, and S. Phadungdhitidhada, "CuO-Cu2O nanocomposite layer for light-harvesting enhancement in ZnO dye-sensitized solar cells," *Applied Surface Science*, 474, pp. 85-90, 2019.

[18] M. Mazloum-Ardakani, and R. Arazi, "Enhancement of photovoltaic performance using a novel photocathode based on poly (3, 4-ethylenedioxythiophene)/Ag–CuO nanocomposite in dye-sensitized solar cell," *Comptes Rendus. Chimie*, vol.23, no. 2, pp. 105-115, 2020.

[19] K. Sharma, V. Sharma, and S. S. Sharma, "Dye-sensitized solar cells: fundamentals and current status," *Nanoscale research letters*, vol. 13, no. 1, pp. 1-46, 2018.

[20] S. Baturay, A. Tombak, D. Batibay, and Y. S. Ocak, "n-Type conductivity of CuO thin films by metal doping," *Appl. Surf. Sci*., vol. 477, pp. 91–95, 2019.

[21] T. Chtouki et al., "Characterization and third harmonic generation calculations of undoped and doped spin-coated multilayered CuO thin films," *J. Phys. Chem. Solids*, vol. 124, pp. 60–66, 2019.

[22] R. Jayakrishnan, A. S. Kurian, V. G. Nair, and M. R. Joseph, "Effect of vacuum annealing on the photoconductivity of CuO thin films grown using sequential ionic layer adsorption reaction," *Mater. Chem. Phys*., vol. 180, pp. 149–155, 2016.

[23] K. Akimoto, S. Ishizuka, M. Yanagita, Y. Nawa, G. K. Paul, and T. Sakurai, "Thin film deposition of Cu2O and application for solar cells," *Sol. Energy*, vol. 80, no. 6, pp. 715–722, 2006.

[24] M. Harada, M. Kuwa, R. Sato, T. Teranishi, M. Takahashi, and S. Maenosono, "Cation distribution in monodispersed MFe_2O_4 (M= Mn, Fe, Co, Ni, and Zn) nanoparticles investigated by x-ray absorption fine structure spectroscopy: implications for magnetic data storage, catalysts, sensors, and ferrofluids," *ACS Applied Nano Materials*, vol. 3, no. 8, pp. 8389–8402, 2020.

[25] C. H. Tsai, P. H. Fei, C. M. Lin, and S. L. Shiu, "CuO and CuO/graphene nanostructured thin films as counter electrodes for Pt-free dye-sensitized solar cells," *Coatings*, vol. 8, no. 1, p. 21, 2018.

[26] N. Abraham, A. Rufus, C. Unni, and D. Philip, "Dye sensitized solar cells using catalytically active CuO-ZnO nanocomposite synthesized by single step method," *Spectrochimica Acta Part A: Molecular and Biomolecular Spectroscopy*, 200, pp. 116-126, 2018.

[27] J. K. Sharma, M.S. Akhtar, S. Ameen, P. Srivastava, and G. Singh, "Green synthesis of CuO nanoparticles with leaf extract of Calotropis gigantea and its dye-sensitized solar cells applications," *Journal of Alloys and Compounds*, 632, pp. 321-325, 2015.

[28] V. S. Prabhin, K. Jeyasubramanian, N. R. Romulus, and N. N. Singh, "Fabrication of dye sensitized solar cell using chemically tuned CuO nano-particles prepared by sol-gel method," *Archives of Materials Science*, vol. 6, no. 7, pp. 5-9, 2017.

[29] H. Guo, and A. S. Barnard, "Naturally occurring iron oxide nanoparticles: morphology, surface chemistry and environmental stability," *Journal of Materials Chemistry A*, vol. 1, no. 1, pp. 27-42, 2013.

[30] H. Dotan, K. Sivula, M. Grätzel, A. Rothschild, and S. C. Warren, "Probing the photoelectrochemical properties of hematite (α-Fe_2O_3) electrodes using hydrogen peroxide as a hole scavenger," *Energy & Environmental Science*, vol. 4, no. 3, pp. 958-964, 2011.

[31] Y. H. Chen, and C. C. Lin, "Effect of nano-hematite morphology on photocatalytic activity," *Physics and Chemistry of Minerals*, 41, pp. 727-736, 2014.

[32] S. Yang, Y. Xu, Y. Sun, G. Zhang, and D. Gao, "Size-controlled synthesis, magnetic property, and photocatalytic property of uniform α-Fe2O3 nanoparticles via a facile additive-free hydrothermal route," *CrystEngComm*, vol. 14, no. 23, pp. 7915-7921, 2012.

[33] X. L. Fang, C. Chen, M. S. Jin, Q. Kuang, Z. X. Xie, S. Y. Xie, L. S. Zheng, "Single-crystal-like hematite colloidal nanocrystal clusters: synthesis and applications in gas sensors, photocatalysis and water treatment," *Journal of Materials Chemistry,* vol. 19, no. 34, pp. 6154-6160, 2009.

[34] S. K. Patel, D. Agravat, O. Alsalman, J. Surve, I. Crowe, S. Taya, and T. K. Nguyen, "Design of a broadband solar absorber based on Fe_2O_3/CuO thin film absorption structure," *Optical and Quantum Electronics*, vol. 55, no. 5, p. 430, 2023.

[35] D. Yang, C. Bai, J. Liu, S. Li, C. Tu, F. Zhu, and T. Zhang, "Construction of 3DOM Fe2O3/CuO heterojunction nanomaterials for enhanced AP decomposition," *Applied Surface Science,* 619, p. 156739, 2023.

[36] H. Alnahari, A. H. Al-Hammadi, A. Al-Sharabi, A. Alnehia, and A. B. Al-Odayni, "Structural, morphological, optical, and antibacterial properties of $CuO–Fe_2O_3–MgO–CuFe_2O_4$ nanocomposite synthesized via auto-combustion route," *Journal of Materials Science: Materials in Electronics*, vol. 34, no. 7,p. 682, 2023.

[37] M. E. Fleet, "The structure of magnetite: Symmetry of cubic spinels," *J. Solid State Chem.*, vol. 62, no. 1, pp. 75–82, 1986.

[38] D. Varshney and A. Yogi, "Structural and transport properties of stoichiometric and Cu2+-doped magnetite: $Fe_{3-x}Cu_xO_4$," *Materials Chemistry and Physics*, vol. 123, no. 2–3, pp. 434–438, 2010.

[39] F. J. Owens, and J. Orosz, "Effect of nanosizing on lattice and magnon modes of hematite," *Solid state communications*, vol. 138, no.2, pp. 95-98, 2006.

[40] A. M. Jubb and H. C. Allen, "Vibrational spectroscopic characterization of hematite, maghemite, and magnetite thin films produced by vapor deposition," *ACS Applied Materials and Interfaces*, vol. 2i no. 10, pp. 2804-2812, 2010.

[41] F. A. Akgul, G. Akgul, N. Yildirim, H. E. Unalan, and R. Turan, "Influence of thermal annealing on microstructural, morphological, optical properties and surface electronic structure of copper oxide thin films," *Mater. Chem. Phys.*, vol. 147, no. 3, pp. 987–995, 2014.

[42] A. M. Jubb and H. C. Allen, "Vibrational spectroscopic characterization of hematite, maghemite, and magnetite thin films produced by vapor deposition," *ACS Appl. Mater. Interfaces*, vol. 2, no. 10, pp. 2804–2812, 2010.